ADVANCED MATERIALS
www.advmat.de

A Highly Efficient Self-Healing Elastomer with Unprecedented Mechanical Properties

*Luzhi Zhang, Zenghe Liu, Xueli Wu, Qingbao Guan, Shuo Chen, Lijie Sun, Yifan Guo, Shuliang Wang, Jianchun Song, Eric Meade Jeffries, Chuanglong He, Feng-Ling Qing, Xiaoguang Bao, and Zhengwei You**

It is highly desirable, although very challenging, to develop self-healable materials exhibiting both high efficiency in self-healing and excellent mechanical properties at ambient conditions. Herein, a novel Cu(II)–dimethylglyoxime–urethane-complex-based polyurethane elastomer (Cu–DOU–CPU) with synergetic triple dynamic bonds is developed. Cu–DOU–CPU demonstrates the highest reported mechanical performance for self-healing elastomers at room temperature, with a tensile strength and toughness up to 14.8 MPa and 87.0 MJ m^{-3}, respectively. Meanwhile, the Cu–DOU–CPU spontaneously self-heals at room temperature with an instant recovered tensile strength of 1.84 MPa and a continuously increased strength up to 13.8 MPa, surpassing the original strength of all other counterparts. Density functional theory calculations reveal that the coordination of Cu(II) plays a critical role in accelerating the reversible dissociation of dimethylglyoxime–urethane, which is important to the excellent performance of the self-healing elastomer. Application of this technology is demonstrated by a self-healable and stretchable circuit constructed from Cu–DOU–CPU.

Self-healing is a beneficial feature of biological tissues that enables them to efficiently repair themselves after mechanical injuries.[1] Inspired by nature, introducing this self-healing property into synthetic materials greatly enhances their longevity and stability, reduces their maintenance expenses, and enables novel applications.[2] Thus, self-healing materials have attracted significant attention and showed great promise in many fields such as automotive coating, electronic skin, and soft robotic.[3] Self-healing materials based on extrinsic healing reagents pioneered this field two decades ago. However, their limited healing ability due to the exhaustion of healing reagents limits their wide applications.[4] Accordingly, the current active research has been shifted to intrinsic healing materials based dynamic noncovalent interactions or reversible covalent bonds. However, the self-healing process usually requires external energy input such as heat,[5–9] light,[10,11] pressure,[12] or other agents.[13] Since many materials in real life are damaged at ambient conditions without available external stimuli, it is highly desired to develop materials that can spontaneously self-heal at room temperature.

A common strategy for design materials that heal at room temperature is to incorporate dynamic noncovalent interactions such as hydrogen bonds,[14–17] metal–ligand coordination,[18–20] host–guest interactions,[21] ionic interactions,[22,23] and van der Waals forces.[24,25] A small amount of noncovalent interactions may lead to good self-healing. However, the resultant materials are usually relatively weak. In contrast, a large number of noncovalent interactions may lead to better mechanical properties, but would likely compromise the self-healing, stretchability and toughness of materials. Furthermore, due to their linear molecular structures, these materials may suffer from limited resilience and potential creep. Accordingly, some researchers have chemically cross-linked structures based on dynamic covalent bonds such as urea bonds,[26,27] boron—oxygen bonds,[28–30] and disulfide bonds,[31,32] to build relatively strong healable materials. However, the cross-linked networks restrict the motion of chains and reduce the healing ability. Overall, the self-healing ability and mechanical properties of materials are mutually exclusive in nature. It remains a formidable challenge to simultaneously achieve high mechanical robustness and healing efficiency especially at ambient conditions, since their demands on molecular structures are typically contradictory.[23,32–34]

L. Zhang, Prof. Q. Guan, S. Chen, L. Sun, Y. Guo, S. Wang, J. Song, Prof. Z. You
State Key Laboratory for Modification of Chemical Fibers and Polymer Materials
International Joint Laboratory for Advanced Fiber and Low-Dimension Materials
College of Materials Science and Engineering
Donghua University
Shanghai 201620, P. R. China
E-mail: zyou@dhu.edu.cn

Z. Liu, Prof. C. He, Prof. F.-L. Qing
College of Chemistry
Chemical Engineering and Biotechnology
Donghua University
Shanghai 201620, P. R. China

X. Wu, Prof. X. Bao
College of Chemistry
Chemical Engineering and Materials Science
Soochow University
Suzhou, Jiangsu 215123, P. R. China

Dr. E. M. Jeffries
6120 Fillmore Place
Apt 2, West New York, NJ 07093, USA

The ORCID identification number(s) for the author(s) of this article can be found under https://doi.org/10.1002/adma.201901402.

DOI: 10.1002/adma.201901402

Here we present a new strategy to simultaneously enhance the self-healing and mechanical properties of polymeric materials. The key is Cu–dimethylglyoxime–urethane (Cu–DOU) coordination complex, which builds a covalently cross-linked polyurethane (CPU) elastomer with triple dynamic bonds, termed Cu–DOU–CPU (**Figure 1**A). First, DOU–CPU provides a new room temperature self-healing dual dynamic network consisting of reversible DOU bonds and hydrogen bonds.[6] Then, the introduction of copper ions forms Cu–DOU coordination complexes based on a third dynamic network. More importantly, experiments and density functional theory (DFT) calculations demonstrate that the copper ions can significantly facilitate the dynamic exchange of DOU bonds. The synergetic effect of Cu–DOU based triple hybrid networks significantly improve the performance of the materials, producing unprecedented tensile strength and toughness among all room temperature self-healing elastomers.[14–23,25–29,31–33,35]

Cu–DOU–CPU hybrid networks were readily synthesized by one-pot polycondensation from commercially available polytetramethylene ether glycol (PTMEG), isophorone diisocyanate (IPDI), glycerol, dimethylglyoxime (DMG), and $CuCl_2$, in the presence of catalyst dibutyltin dilaurate. PTMEG is selected as the soft segment because its chain is flexible and can facilitate the chain motion for better self-healing. IPDI is selected as the hard segment, because its bulky structure inhibits the crystallization and increase the chain mobility for better self-healing. Furthermore, IPDI derived urethane has relatively high dynamic due to the steric influence of the cyclohexyl ring, which would further facilitate the reconstruction of covalent networks.[36] Triple-functional glycerol yields covalent cross-linked networks. DMG is the key in the design of Cu–DOU–CPU. DMG acts as the chain extender to introduce reversible DOU groups, crucial for the dynamic covalent networks. Moreover, the methyl groups in DMG inhibit the crystallization of the hard segment and facilitate the chain motion. Furthermore, DMG contains adjacent oxime groups, the nitrogen atoms of which can readily chelate metal ions such as Cu^{2+} from $CuCl_2$ to form a complex. Accordingly, Cu–DOU–CPU contains triple dynamic bonds including reversible DOU covalent bonds, Cu—DOU coordination bonds, and hydrogen bonds. The dissociation of the weaker bonds (hydrogen bonds and Cu—DOU coordination bonds) can significantly dissipate energy during mechanical deformation leading to high toughness. Their reassociation results in efficient self-healing. The relatively strong covalent bonds ensure the structural integration for stable mechanical performance. At the same time, coordination of copper ions promotes the exchange reaction of DOU groups to facilitate the self-healing for eventual mechanical restoration upon being damaged. Overall, the synergetic effect of hybrid triple networks ensures outstanding self-healing and mechanical properties simultaneously (Figure 1B).

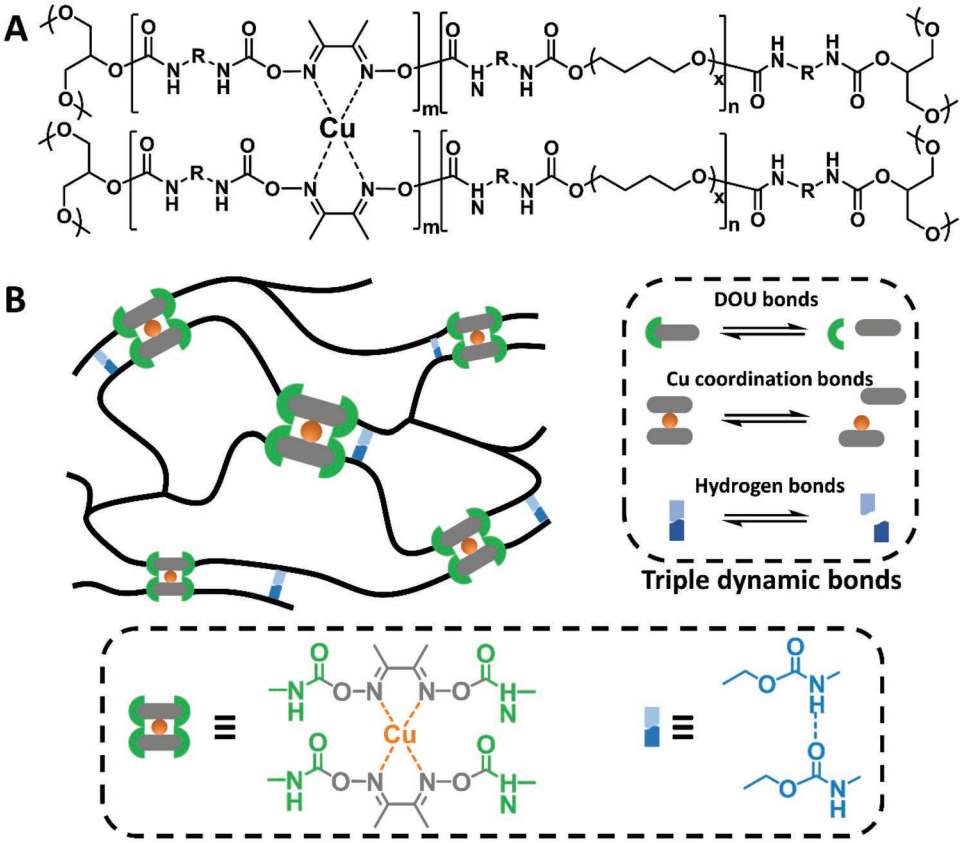

Figure 1. Design of Cu–DOU–CPU elastomer with superior mechanical and self-healing properties. A) Molecular structure of Cu–DOU–CPU elastomer. B) Schematic structure of Cu–DOU–CPU elastomer. Triple dynamic bonds including reversible covalent (green arc and gray stick), metal–ligand (gray stick and orange circle), and hydrogen bonds (blue polygons) constructed hybrid dynamic networks.

As mentioned above, the Cu^{2+} facilitated dynamic exchange reaction of DOU groups and is the key of our design. To verify this reaction we utilized model small molecules, (Figure S1A, Supporting Information). Real-time nuclear magnetic resonance (NMR) monitored the reaction of compound **ab** and **c** to **ac** and **b** with (experimental group) and without (control group) $CuCl_2$ and in the presence of the same amount of catalyst dibutyltin dilaurate at room temperature. The signals at 3.62 ppm in ^1H NMR spectrum and 42.25 ppm in ^{13}C NMR spectrum corresponded to the protons (marked as **ac**-H*) and carbons (marked as **ac**-C*) at the methylene groups near the nitrogens (Figure S1B, Supporting Information), respectively (Figures S2–S5, Supporting Information). Significant **ac**-H* and **ac**-C* signals were observed in the experimental group within half-hour. However, the **ac**-H* and **ac**-C* signals were still weak in the control group after 1 h. In the whole experimental period (20 h), **ac**-H* and **ac**-C* signals of the experimental group were always stronger than the ones of control group. These results suggested that the exchange reaction rate of the experimental group was faster than that of the control group and demonstrated that the presence of copper ions facilitated the dynamic exchange reactions of DOU groups.

In order to further reveal the catalytic role of $CuCl_2$ in the dynamic dissociation/association of DOU bonds, computational studies were carried out to provide a mechanistic insight (**Figure 2**A). It should be noted that **A** can behave as a ligand to coordinate with transition metals. In the presence of $CuCl_2$, four possible structural conformers binding with **A** were optimized, including tetra-, penta-, and hexa-coordinated copper complexes (Figure 2B). Computational results show that the complex, **INT1**, is more favorable than the other three structures, in which a pentacoordinate copper complex is formed. The coordination of the two imino groups with Cu^{2+} can compensate the penalty of steric hindrance caused by the two adjacent methyl groups. In addition, structural examination of **INT1** indicates that the one DOU moiety of **A** can coordinate with Cu^{2+} via the carbonyl group and the other has to distort considerably due to the presence of the catalyst, suggesting that the noncoordinated DOU moiety could be destabilized. The subsequent dissociation of the destabilized DOU moiety of **INT1** was located as **TS1**, in which the breaking of C—O bond accompanies with the proton migration from N to O to produce **INT2** and isocyanate. The predicted free energy barrier is 34.5 kcal mol^{-1} (Figure 2A), which is significantly lower than that without the catalyst (Figure S6, Supporting Information). It should be noted that the formed complex, **INT2**, along with the dissociated isocyanate, is almost thermodynamically neutral. Further fragmentation of **INT2** to yield **INT3** + isocyanate was also investigated. Computational results imply that the $\Delta G^{\neq}$ required for further fragmentation is 3 kcal mol^{-1} higher than that for the reverse association reaction between **INT2** and the isocyanate. Thus, dynamic dissociation/association equilibrium could be established in the presence of $CuCl_2$ catalyst.

The structure of Cu–DOU–CPU was characterized by attenuated total reflectance Fourier transform infrared spectroscopy (ATR-FTIR). The peaks at 3318 and 1713 cm^{-1} corresponded to N—H and C=O stretching vibrations, respectively, indicating the formation of urethane groups. And there were negligible peaks at 2264 and 1222 cm^{-1} (Figure S7, Supporting Information), which corresponded to N=C=O and acetone molecular skeleton stretching vibration, respectively. This revealed that the monomer IPDI had completely reacted, and solvent acetone was completely removed. Accordingly, the self-healing property of Cu–DOU–CPU was not caused by solvent action or residual monomers.

The thermal properties of Cu–DOU–CPU was investigated by dynamic mechanical analysis (DMA) (Figure S8, Supporting Information). The glass transition temperature (T_g) of Cu–DOU–CPU was found at −72.9 °C. Furthermore, X-ray

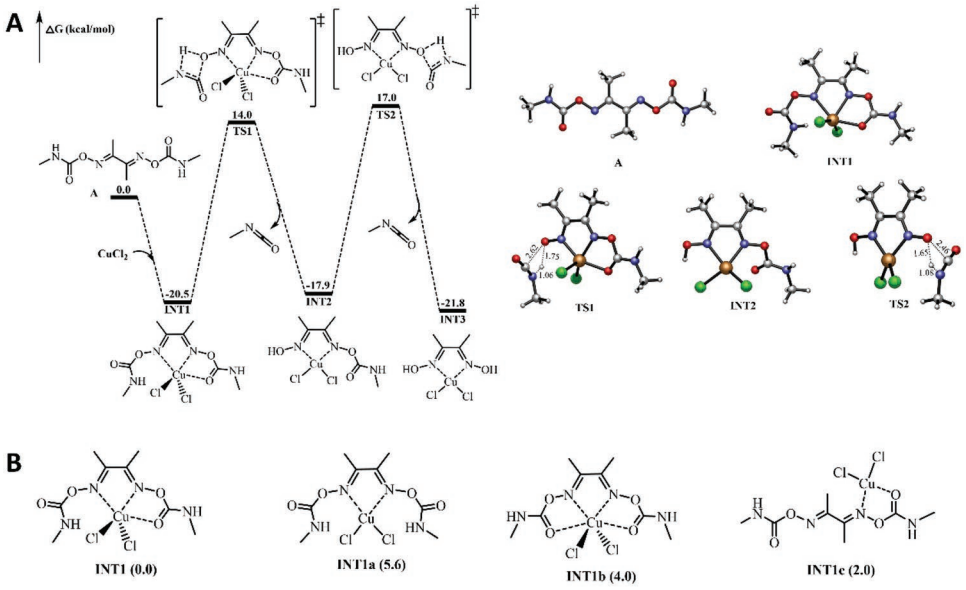

Figure 2. A) Energy profile for the $CuCl_2$-catalyzed dissociation of DOU bonds of **A**. Bond lengths are shown in Å. B) The four possible structural conformers of **A**-$CuCl_2$ complex. The relative energies (in kcal mol^{-1}) are shown in parenthesis.

diffraction (XRD) spectra showed no crystallization peak before and after being stretched (Figure S9, Supporting Information). The swelling experiment without dissolution confirmed the cross-linked structure of Cu–DOU–CPU (Figure S10, Supporting Information).

The self-healing behavior of materials is usually closely related to their surface structure. Thus, narrow X-ray photoelectron spectroscopy (XPS) was used to analyze the surface chemistry of DOU–CPU and Cu–DOU–CPU (**Figure 3**A,B; Figure S11, Supporting Information). Cu–DOU–CPU showed a higher intensity of N 1s than DOU–CPU, indicating more DOU groups existed on Cu–DOU–CPU surface, which likely due to the enhanced mobility of DOU groups in Cu–DOU–CPU compared to DOU–CPU. More DOU groups could promote the self-healing process. The peak at 933.9 eV was attributed to copper coordination complex. The shake-up peaks at 940.9–943.9 and 962.8 eV indicated the presence of partly coordinated copper ions. The copper on the surface of the Cu–DOU–CPU can also facilitate the exchange reaction of DOU groups and Cu—DOU coordination bonds to further promote healing.

Next, the self-healing properties of Cu–DOU–CPU were characterized in detail. A surface scratch recovery test was first performed. A blade made 30–50 µm wide scratches on a Cu–DOU–CPU film. Optical microscopy images showed

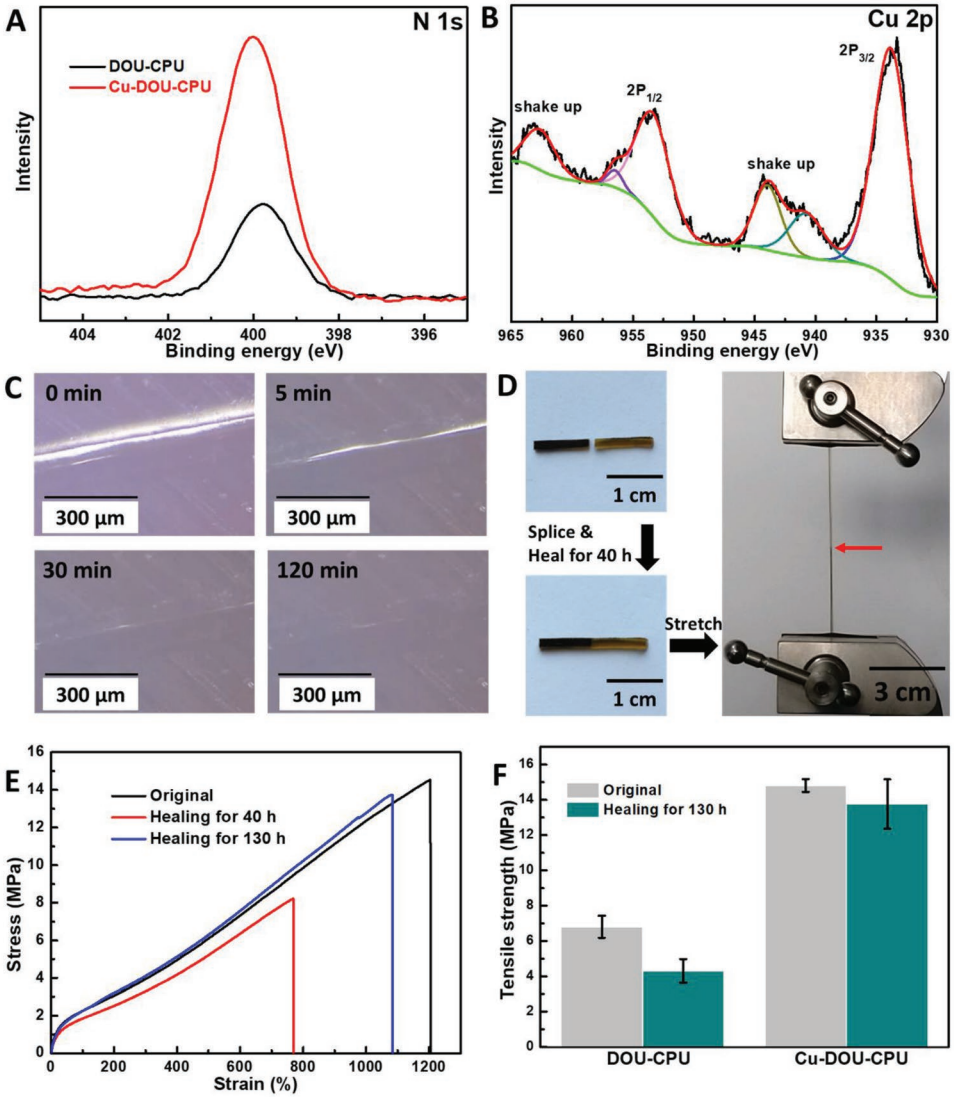

Figure 3. Self-healing properties of the Cu–DOU–CPU elastomer. A) XPS spectra of N 1s region of DOU–CPU and Cu–DOU–CPU and B) Cu 2p region of Cu–DOU–CPU. The higher N 1s intensity indicated more DOU groups on Cu–DOU–CPU surface for better healing. Furthermore, the copper ions on the surface of the Cu–DOU–CPU could also promote the exchange reaction of DOU groups and Cu—DOU coordination bonds further promote healing. C) Optical microscopy images of Cu–DOU–CPU film after being scratched. It showed a rapid self-healing with an almost complete recovery within 2 h at room temperature. D) Photographs of bulky self-healing process of Cu–DOU–CPU. The Cu–DOU–CPU strip was cut into two pieces and one was stained black before rejoining again under ambient conditions. After 40 h, the strip was readily stretched to over 800%. The red arrow referred to the healing area. E) Typical tensile stress–strain curves of original and healed (healing for 40 and 130 h at room temperature) Cu–DOU–CPU. F) Tensile strength of original and healed (healing for 130 h at room temperature) DOU–CPU and Cu–DOU–CPU. Cu–DOU–CPU showed a much better self-healing than DOU–CPU.

near complete self-healing within 2 h at room temperature (Figure 3C). The bulky self-healing of Cu–DOU–CPU was also evaluated. The strip was cut into two pieces. One was stained black and the two were rejoined under ambient conditions. The strips began to heal immediately likely due to noncovalent interactions. The instant self-healing properties were assessed after just 30 s (Figure S12, Supporting Information). The toughness of healed Cu–DOU–CPU (4.26 ± 0.76 MJ m^{-3}) was over 4 times that of healed DOU–CPU (0.96 ± 0.06 MJ m^{-3}). The tensile strength of healed Cu–DOU–CPU (1.84 ± 0.05 MPa) was almost twice that of healed DOU–CPU (0.98 ± 0.12 MPa) and already comparable to the original tensile strength of lots of reported room temperature self-healing elastomers.[15,18–21,26,27,31,33,35] This indicated that Cu–DOU coordination interaction played an important role in rapid self-healing in addition to hydrogen bonds. Then the mechanical properties steadily recovered with the reformation of both noncovalent bonds and covalent DOU bonds. The short-term self-healing ability was evaluated after 2 h (Figure S13, Supporting Information). After 40 h (Figure 3D), its toughness and tensile strength recovered to 38.1 ± 6.0 MJ m^{-3} and 8.0 ± 0.4 MPa (Figure 3E), exceeding the original tensile toughness and strength of almost all reported room temperature self-healing elastomers.[14,15,17–22,25–29,31–33,35] By extending the healing time to 130 h, the mechanical properties of the Cu–DOU–CPU were significantly improved further with a world-record tensile strength of room temperature self-healing elastomers up to 13.8 ± 1.4 MPa, dramatically higher than the one of DOU–CPU (6.8 ± 0.6 MPa). Even the relative recovery rate of Cu–DOU–CPU (92% ± 9%) was greatly higher than that of DOU–CPU (63% ± 10%) (Figure 3F). Although Cu–DOU–CPU showed a similar self-healing efficiency to that of DOU–CPU at early stage, its absolute tensile strength was much higher than that of DOU–CPU (Figure S13, Supporting Information). At later stage, the reconstruction of covalent network predominated self-healing process leading to a much better healing of Cu–DOU–CPU compared to DOU–CPU. These results clearly demonstrated that the introduction of Cu^{2+} significantly promote the self-healing.

As designed, the copper-mediated triple networks not only facilitated the self-healing but also strengthened Cu–DOU–CPU elastomer. Next, we discuss the detailed mechanical properties and mechanisms (**Figure 4**A). Covalent cross-links fix the polymer networks. Dynamic cross-links based on hydrogen bonds and Cu—DOU coordination bonds act as sacrificial bonds that can rupture upon loading to dissipate energy and reform after unloading to restore the structures and mechanical properties. The triple sacrificial bonds system gave Cu–DOU–CPU outstanding mechanical properties.

ATR-FTIR was used to study the Cu—DOU coordination bonds (Figure 4B). The peak corresponding to the N–O stretching vibration of DOU–CPU at 987.8 cm^{-1} shifted to 979.3 cm^{-1} after coordination with cooper ions (Cu–DOU–CPU). With the Cu–DOU–CPU strip being strained to 400% and 800%, the peak shifted from 979.3 to 980.6 and 981.5 cm^{-1}, respectively. When the strip was unloaded and relaxed for 5 min under ambient conditions, the peak shifted back to 979.5 cm^{-1}. These results indicated a rapid association and dissociation of the Cu—DOU coordination bonds during loading and unloading. ATR-FTIR also revealed the evolution of hydrogen bonds in Cu–DOU–CPU (Figure S14, Supporting Information). The spectra of Cu–DOU–CPU had a wide peak at 3330 cm^{-1}, which indicated the existence of a large number of hydrogen bonded N–H groups. When the Cu–DOU–CPU was increased strain to 400% and 800%, the peak at 3330 cm^{-1} became narrower and weaker indicating the rupture of hydrogen bonds. After unloading and relaxing for 5 min, the peak at 3330 cm^{-1} became wider and stronger indicating the reformation of hydrogen bonds.

In order to further understand the role of Cu—DOU coordination bonds in Cu–DOU–CPU system, we used dynamic mechanical analysis to carry out stress relaxation modulus tests for DOU–CPU and Cu–DOU–CPU at room temperature (Figure 4C). The characteristic relaxation time (τ^*) defined as the time required for $G/G_0 = 1/e$, measures the speed of the polymer chain rearrangement. Due to the cross-links formed by the Cu–DOU coordination complex, Cu–DOU–CPU (τ^* = 146.3 s) showed a longer relaxation time than DOU–CPU (τ^* = 59.2 s). As designed, the coordination of copper ions would strengthen and toughen the resultant hybrid networks by increasing dynamic cross-link points and consequent energy dissipation of their reversible rupture upon loading. The tensile strength and toughness of Cu–DOU–CPU (14.8 ± 0.4 MPa and 87.0 ± 6.3 MJ m^{-3}) were more than twice that of DOU–CPU (6.8 ± 0.6 MPa and 39.0 ± 1.6 MJ m^{-3}) (Figure 4D) and significantly higher than all the reported room temperature self-healing elastomers (Figure 4H).[14–23,25–29,31–33,35] At the same time, the elongation at break of Cu–DOU–CPU approached 1182% ± 68% (Figure 4G) which was much higher than that for DOU–CPU (901% ± 45%). This was likely due to increased hidden length of more folded polymer chains caused by Cu—DOU coordination bonds.[37]

The dual sacrificial bonds and covalent networks of Cu–DOU–CPU was expected to endow it with a high toughness and good elasticity, respectively. We performed cyclic tensile test to further evaluate these properties. Firstly, cyclic tensile tests of Cu–DOU–CPU were performed with gradually larger strains. In the sequential cyclic tensile test (Figure 4E), there was no waiting time between two consecutive loadings. After the first tensile cycle with a small strain (100%), the covalent networks and the unbroken dynamic bonds (hydrogen bonds and Cu—DOU coordination bonds) entropically drove the networks almost back to its original state. This revealed Cu–DOU–CPU was a good elastomer within the strain up to 100%, feasible for many practical applications. After sequential cycles with larger strains (≥200%), Cu–DOU–CPU showed observable residual strain, due to the reformation of broken dynamic bonds at new sites during stretching. The hysteresis loops of curves indicated successful energy dissipation of Cu–DOU–CPU. Secondly, to demonstrate the elastic performance of Cu–DOU–CPU, repeated cyclic tensile tests at a large strain of 500% were performed (Figure 4F). There was no waiting time between two consecutive cyclic tests for ten cycles. There was a large hysteresis loop in first cycle indicating a significant energy dissipation. The energy dissipation in second cycle was much less than that in first cycle because the broken sacrificial bonds did not have enough time to restore to their original state during the limited timeframe. The hysteresis loop slightly decreased with the increase of cycle in sequential test,

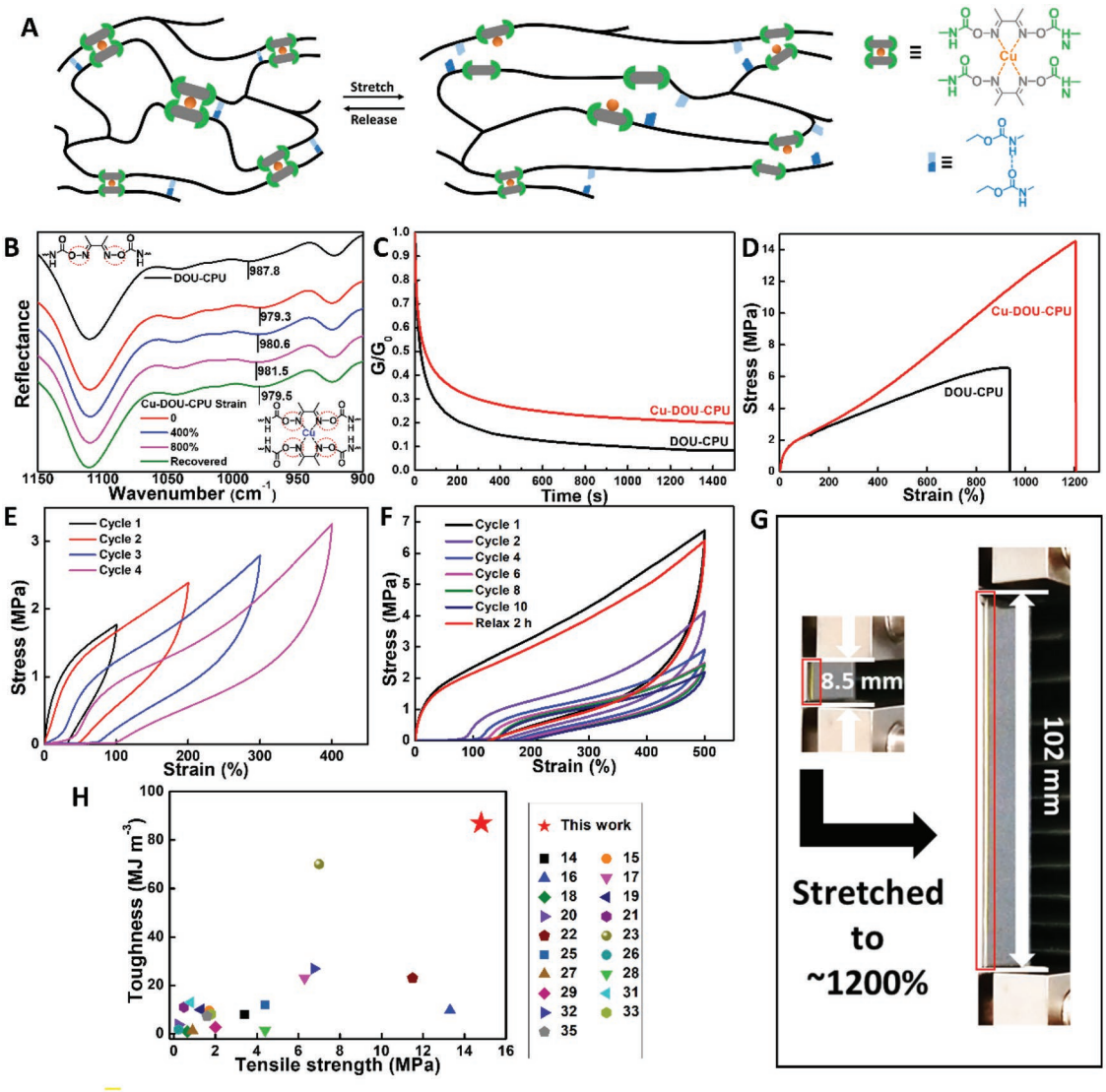

Figure 4. Mechanical properties of the Cu–DOU–CPU elastomer. A) Proposed mechanism of bond rupture and reformation in Cu–DOU–CPU during stretching. The covalent bonds kept intact before and after being stretched. The hydrogen bonds and Cu—DOU coordination bonds served as sacrificial bonds that could rupture during stretching to dissipate energy and reform after release. B) ATR-FTIR spectra of DOU–CPU and Cu–DOU–CPU under various strains. The characteristic peak assigned to the N–O (in dotted red circle) stretching vibration bond was marked out. With the Cu–DOU–CPU strip being increased strain to 400% and 800%, the peak shifted from 979.3 to 980.6 and 981.5 cm^{-1}, respectively. When the strip was relaxed for 5 min under ambient conditions, the peak shifted back to 979.5 cm^{-1}. C) Normalized stress-relaxation analysis of DOU–CPU and Cu–DOU–CPU under ambient temperature. Cu–DOU–CPU showed a longer relaxation time than DOU–CPU. D) Tensile stress–strain curves of DOU–CPU and Cu–DOU–CPU. E) Sequential cyclic tensile curves of Cu–DOU–CPU at different strains without waiting time between two consecutive loadings. It showed successful recovery of elastic modulus and limited residual strain for strain <200% within limited testing time. F) Repeated cyclic tensile curves of Cu–DOU–CPU at 500% strain. There was no waiting time between two consecutive cyclic tensile (cycle 1-cycle 10). The film was then allowed to relax for 2 h at 25 °C before the 11th cyclic tensile test. Cycle 11 showed a similar loading–unloading curve to that of cycle 1, indicating that Cu–DOU–CPU almost fully recovered its original tensile behavior. G) Photographs of Cu–DOU–CPU strip (marked by red rectangle) before and after being stretched showed its high stretchability. H) Ashby plot of "toughness" and "tensile strength" of Cu–DOU–CPU and other room temperature self-healing elastomers reported in literatures.[14–23,25–29,31–33,35] Cu–DOU–CPU exhibited the highest tensile strength and toughness simultaneously.

indicating the continuous reorganization of sacrificial bonds. When the sample was allowed to relax for 2 h at 25 °C and subjected to the 11th cyclic tensile, it showed a loading–unloading curve similar to that of the first cycle, indicating good elastic recovery of Cu–DOU–CPU. A further cyclic test for more cycles (Figure S15, Supporting Information) and at different strain rate (Figure S16, Supporting Information) showed a similar trend.

As a preliminary demonstration, we used Cu–DOU–CPU to build a stretchable and self-healable conductor, which is very important for next generation flexible electronics, but still remains a great challenge.[38] The composite conductor used Cu–DOU–CPU as the sheath and gallium indium tin eutectic as the core (**Figure 5**A). A circuit with this conductor and 3 V voltage batteries efficiently illumed a connected light-emitting

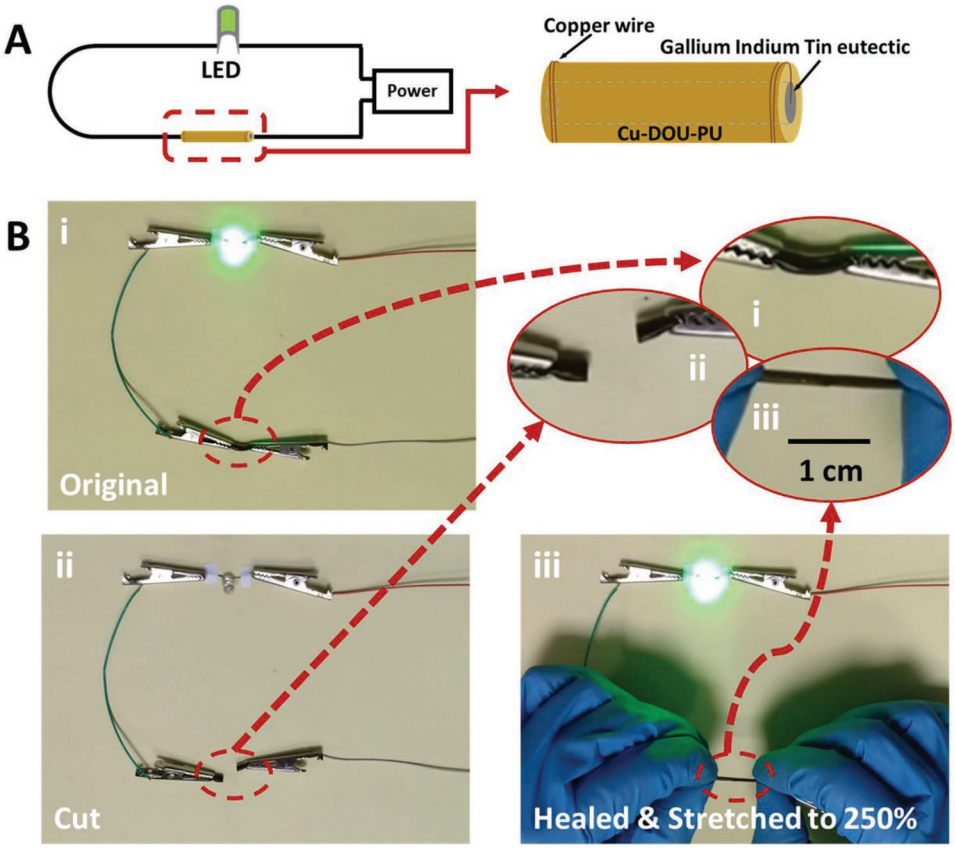

Figure 5. Rapidly self-healing and stretchable composite conductor. A) Schematics illustrating the simple electronic circuit and the composite conductor. B) Demonstration of the self-healing and stretchable properties for the composite conductor in series with an LED. i,ii) The LED was lit at the original stage (i), and turned off after the conductor being cut (ii). iii) The severed composite conductor was efficiently healed within 9 min under ambient conditions. The healed conductor kept the LED on even while being stretched to 250%.

diode (LED). When the composite conductor was cut to two pieces, the LED was off. Within 9 min, the two cut pieces readily self-healed without any external stimuli and the LED turned back on. This is significantly faster than some recently reported self-healed conductors, which required hours to heal.[33,39,40] Furthermore, the healed composite conductor could be stretched to 250% while the LED was still on (Figure 5B). In view of the superior mechanical properties of Cu–DOU–CPU, the conductor may be used for demanding applications. For example, wires are an important integral part of all electronic equipment. The corresponding cable sheaths (T11, T14, etc.) usually need high tensile strength over 12.5 MPa according to European and Chinese standards. Unfortunately, there is no previously reported room temperature self-healing materials with such high mechanical strength. The tensile strength of Cu–DOU–CPU was 14.8 ± 0.4 MPa, and would be a promising candidate. Overall, the composite conductor has excellent mechanical properties and self-healing ability superior to recently reported counterparts.[32,33] In addition, Cu–DOU–CPU showed good insulation properties with a high resistivity (1.46×10^8 Ω m), feasible for practical application.

In summary, we designed and synthesized a new room temperature self-healing material Cu–DOU–CPU, with outstanding mechanical properties. Cu–DOU–CPU exhibits an initial (14.8 MPa) and healed (13.8 MPa) tensile strength, both of which exceed the highest initial tensile strength (13.3 MPa) of previously reported room temperature self-healing elastomers.[14–23,25–29,31–33,35] Similarly, it is tougher (87.0 MJ m^{-3}) than the current state of the art room temperature self-healing elastomer (70 MJ m^{-3}).[23] The key to achieving these properties is the synergistic effect of triple dynamic bonds including reversible DOU bonds, Cu—DOU coordination bonds, and hydrogen bonds. The introduction of Cu—DOU coordination bonds especially strengthened and toughened the materials while also enhancing the dynamics of adjacent DOU bonds, which was confirmed by DFT calculations. This material design provides a powerful new strategy to reconcile the traditionally contradictory properties of mechanical robustness and self-healing efficiency that can also be expanded to other metal ions and dynamic bonds. In addition, the synthesis of Cu–DOU–CPU elastomer is a simple one step process using commercially available reagents that can be readily scaled up. We expect our approach to inspire a series of strong self-healing materials with applications in fields such as protective coatings, soft robotics, and wearable electronics.

Supporting Information

Supporting Information is available from the Wiley Online Library or from the author.

Acknowledgements

L.Z. and Z.L. contributed equally to this work. This work was financially supported by the National Natural Science Foundation of China (21574019, 21642004, 31570984, and 31771048), the Natural Science Foundation of Shanghai (18ZR1401900), International Joint Laboratory for Advanced fiber and Low-dimension Materials (18520750400), the Fundamental Research Funds for the Central Universities, DHU Distinguished Young Professor Program (LZA2019001), and the Science and Technology Commission of Shanghai (17DZ2260100).

Conflict of Interest

The authors declare no conflict of interest.

Keywords

dynamic covalent bonds, elastomers, metal coordination, polyurethane, self-healing

Received: March 3, 2019
Revised: March 26, 2019
Published online:

[1] C. E. Diesendruck, N. R. Sottos, J. S. Moore, S. R. White, *Angew. Chem., Int. Ed.* **2015**, *54*, 10428.
[2] Z. P. Zhang, M. Z. Rong, M. Q. Zhang, *Prog. Polym. Sci.* **2018**, *80*, 39.
[3] S. Wang, J. Y. Oh, J. Xu, H. Tran, Z. Bao, *Acc. Chem. Res.* **2018**, *51*, 1033.
[4] J. F. Patrick, M. J. Robb, N. R. Sottos, J. S. Moore, S. R. White, *Nature* **2016**, *540*, 363.
[5] X. Chen, M. A. Dam, K. Ono, A. Mal, H. Shen, S. R. Nutt, K. Sheran, F. Wudl, *Science* **2002**, *295*, 1698.
[6] W. X. Liu, C. Zhang, H. Zhang, N. Zhao, Z. X. Yu, J. Xu, *J. Am. Chem. Soc.* **2017**, *139*, 8678.
[7] Y. Lai, X. Kuang, P. Zhu, M. Huang, X. Dong, D. Wang, *Adv. Mater.* **2018**, *30*, 1802556.
[8] M. Röttger, T. Domenech, R. van der Weegen, A. Breuillac, R. Nicolaÿ, L. Leibler, *Science* **2017**, *356*, 62.
[9] T. Defize, J. M. Thomassin, M. Alexandre, B. Gilbert, R. Riva, C. Jerome, *Polymer* **2016**, *84*, 234.
[10] M. Burnworth, L. Tang, J. R. Kumpfer, A. J. Duncan, F. L. Beyer, G. L. Fiore, S. J. Rowan, C. Weder, *Nature* **2011**, *472*, 334.
[11] P. Song, H. Qin, H. L. Gao, H. P. Cong, S. H. Yu, *Nat. Commun.* **2018**, *9*, 2786.
[12] Y. Yanagisawa, Y. Nan, K. Okuro, T. Aida, *Science* **2018**, *359*, 72.
[13] B. K. Ahn, D. W. Lee, J. N. Israelachvili, J. H. Waite, *Nat. Mater.* **2014**, *13*, 867.
[14] P. Cordier, F. Tournilhac, C. Soulie-Ziakovic, L. Leibler, *Nature* **2008**, *451*, 977.
[15] Y. Chen, A. M. Kushner, G. A. Williams, Z. Guan, *Nat. Chem.* **2012**, *4*, 467.
[16] J. Wu, L.-H. Cai, D. A. Weitz, *Adv. Mater.* **2017**, *29*, 1702616.
[17] Y. Wang, X. Liu, S. Li, T. Li, Y. Song, Z. Li, W. Zhang, J. Sun, *ACS Appl. Mater. Interfaces* **2017**, *9*, 29120.
[18] Y. L. Rao, A. Chortos, R. Pfattner, F. Lissel, Y. C. Chiu, V. Feig, J. Xu, T. Kurosawa, X. Gu, C. Wang, M. He, J. W. Chung, Z. Bao, *J. Am. Chem. Soc.* **2016**, *138*, 6020.
[19] D. Mozhdehi, S. Ayala, O. R. Cromwell, Z. Guan, *J. Am. Chem. Soc.* **2014**, *136*, 16128.
[20] C. H. Li, C. Wang, C. Keplinger, J. L. Zuo, L. Jin, Y. Sun, P. Zheng, Y. Cao, F. Lissel, C. Linder, X. Z. You, Z. Bao, *Nat. Chem.* **2016**, *8*, 618.
[21] J. Liu, C. S. Y. Tan, Z. Yu, N. Li, C. Abell, O. A. Scherman, *Adv. Mater.* **2017**, *29*, 1605325.
[22] J. Zhang, M. Huo, M. Li, T. Li, N. Li, J. Zhou, J. Jiang, *Polymer* **2018**, *134*, 35.
[23] Y. Miwa, J. Kurachi, Y. Kohbara, S. Kutsumizu, *Commun. Chem.* **2018**, *1*, 5.
[24] M. W. Urban, D. Davydovich, Y. Yang, T. Demir, Y. Zhang, L. Casabianca, *Science* **2018**, *362*, 220.
[25] A. Susa, R. K. Bose, A. M. Grande, S. van der Zwaag, S. J. Garcia, *ACS Appl. Mater. Interfaces* **2016**, *8*, 34068.
[26] P.-F. Cao, B. Li, T. Hong, J. Townsend, Z. Qiang, K. Xing, K. D. Vogiatzis, Y. Wang, J. W. Mays, A. P. Sokolov, T. Saito, *Adv. Funct. Mater.* **2018**, *28*, 1800741.
[27] H. Ying, Y. Zhang, J. Cheng, *Nat. Commun.* **2014**, *5*, 3218.
[28] J. J. Cash, T. Kubo, A. P. Bapat, B. S. Sumerlin, *Macromolecules* **2015**, *48*, 2098.
[29] Y. Chen, Z. Tang, X. Zhang, Y. Liu, S. Wu, B. Guo, *ACS Appl. Mater. Interfaces* **2018**, *10*, 24224.
[30] T. Wu, B. Chen, *ACS Appl. Mater. Interfaces* **2016**, *8*, 24071.
[31] A. Rekondo, R. Martin, A. Ruiz de Luzuriaga, G. Cabañero, H. J. Grande, I. Odriozola, *Mater. Horiz.* **2014**, *1*, 237.
[32] S.-M. Kim, H. Jeon, S.-H. Shin, S.-A. Park, J. Jegal, S. Y. Hwang, D. X. Oh, J. Park, *Adv. Mater.* **2018**, *30*, 1705145.
[33] Q. Zhang, S. Niu, L. Wang, J. Lopez, S. Chen, Y. Cai, R. Du, Y. Liu, J.-C. Lai, L. Liu, C.-H. Li, X. Yan, C. Liu, J. B.-H. Tok, X. Jia, Z. Bao, *Adv. Mater.* **2018**, *30*, 1801435.
[34] J. C. Lai, L. Li, D. P. Wang, M. H. Zhang, S. R. Mo, X. Wang, K. Y. Zeng, C. H. Li, Q. Jiang, X. Z. You, J. L. Zuo, *Nat. Commun.* **2018**, *9*, 2725.
[35] T. Wang, Y. Zhang, Q. Liu, W. Cheng, X. Wang, L. Pan, B. Xu, H. Xu, *Adv. Funct. Mater.* **2018**, *28*, 1705551.
[36] D. A. Wicks, Z. W. W. Jr., *Prog. Org. Coat.* **2001**, *43*, 131.
[37] G. E. Fantner, T. Hassenkam, J. H. Kindt, J. C. Weaver, H. Birkedal, L. Pechenik, J. A. Cutroni, G. A. G. Cidade, G. D. Stucky, D. E. Morse, P. K. Hansma, *Nat. Mater.* **2005**, *4*, 612.
[38] T.-P. Huynh, P. Sonar, H. Haick, *Adv. Mater.* **2017**, *29*, 1604973.
[39] J. Kang, D. Son, G.-J. N. Wang, Y. Liu, J. Lopez, Y. Kim, J. Y. Oh, T. Katsumata, J. Mun, Y. Lee, L. Jin, J. B.-H. Tok, Z. Bao, *Adv. Mater.* **2018**, *30*, 1706846.
[40] T. Long, Y. Li, X. Fang, J. Sun, *Adv. Funct. Mater.* **2018**, *28*, 1804416.